JOURNAL OF MATERIALS SCIENCE **34** (1999) 5265–5272

Effect of surface pretreatments on the adherence of porcelain enamel to a type 316L stainless steel

F. S. SHIEU, M. J. DENG, K. C. LIN, J. C. WONG
Institute of Materials Engineering, National Chung Hsing University, Taichung 402, Taiwan
J. Y. WU
Institute of Chemical Engineering, National Chung Hsing University, Taichung 402, Taiwan

Porcelain enameled 316L stainless steel with different surface pretreatments was produced by a slurry-fusion technique for evaluation of the enamel/steel adherence using an electrical conductivity meter. From the measured results, it is found that the adherence of the porcelain enamel to the steel depends on the roughness of the enamel-steel interface, which, in turn, is controlled by surface pretreatments of the steel substrates. The difference in the adherence of the enameled steel can be explained from an examination of the microstructure of enamel-steel interfaces by scanning electron microscopy. Good adherence is associated with those specimens that have a long enamel-steel interface contour, i.e., rough interfaces. In addition, X-ray diffraction analysis of the delaminated enamel fragments upon impact deformation reveals that failure of the enamel coatings in an oxidized steel occurred at the oxide-steel interface which is supposed to have strong chemical bonding, and that the oxide scales present before enameling are partially dissolved in the enamel during firing. The difference in the coefficients of thermal expansion among enamel, oxide, and steel is likely to play an important role in determining the failure mode of the enameled stainless steel. In summary, these results suggest that the adherence of the porcelain enamel to the 316L stainless steel is mainly controlled by a mechanism of mechanical interlocking.

1. Introduction

Alloying is an effective means for improving the resistance of iron-based metals to attacks by corrosive environments at either moderate or elevated temperatures [1]. Among the various alloyed low carbon steels, the 18% Cr, 8% Ni (18-8) austenitic stainless steel is the most popular and widely used among the stainless steels now produced. The austenitic stainless steels, in general, are resistance to nitric acids, dilute sulfuric acid at room temperature, most food acids and acetic acid, sulfurous acid, alkalies, and the atmosphere. They are, however, not resistant to dilute or concentrated HCl, HBr, and HF, oxidizing chlorides and seawater, and concentrated sulfuric acid at high temperature. For power and energy applications in which the atmosphere often contains sulfur dioxide at high temperature, it has been found that components made of austenitic stainless steels have very short service life [2].

Application of ceramic coatings to stainless steels is an alternative route to solve the corrosion problem. Among the various ceramic coatings including oxides, nitrides and carbides, porcelain enamel is one of the most economic and well-established technologies. The physical, mechanical, and corrosion resistance, as well as microstructure, of porcelain enameled low carbon steels are well studied [3–7]. In contrast, our understanding of the microstructure and properties of porcelain enameled stainless steel is very limited. From a previous study by Shieu *et al*. [8], it is found that the corrosion resistance of 316L stainless steel was improved markedly by the application of porcelain enamel to the steel. It is the objective of this research to further investigate the effect of surface pretreatments on the interfacial microstructure and the adherence of porcelain enamel to the steel. The predominant bonding mechanism which controls the adherence of the enamel to the stainless steel, is also discussed.

2. Experimental

A commercially available type 316L stainless steel with very low carbon content was used as the substrate for this study. The nominal concentrations of C, Cr, Ni, Mo, Mn, P, Si, and V in the steel were 0.023, 17.26, 11.01, 2.06, 1.715, 0.029, 0.420, and 0.071%, respectively. A total of forty specimens (five in each group) of dimensions $150 \times 100 \times 1.5$ mm were cut from a large stainless steel plate. The two sides of the steel plate had different finishes: one with rolling marks and the other exhibiting optical smoothness. On the basis of initial surface finishes, the specimens for enameling were classified into three categories, i.e., (i) those treated with ball blasting, (ii) as-received specimens of which the surface had rolling marks, and (iii) as-received specimens

TABLE I The experimental conditions and adherence test results of porcelain enameled stainless steel

	Surface treatments of substrates before enameling				
Category	Ball-blasting	Polishing with 1 μm Al_2O_3	Oxidation in air at 500 °C for 5 min	PEI test adherence index	Ratio of interface contour
i	yes			53 ± 13	1.48
ii		yes		74 ± 7	1.27
			yes	54 ± 17	1.34
		yes	yes	54 ± 20	1.29
iii		yes		4.5 ± 2	1.08
			yes	0	1.00
		yes	yes	0	1.04
				2.3 ± 0.6	1.00

of which the surface was optically smooth. Ball blasting was carried out with a mixture of steel balls ranging from 0.1 ∼ 1 mm in diameter at a pressure of 2.0 MPa. For specimens of the last two categories, three different treatments including (a) final polishing with 1 μm Al_2O_3 powder, (b) oxidation in air at 500 °C for 5 min, and (c) a combination of (a) and (b), were further implemented. The as-prepared specimens were subjected to degreasing in a 5% Na_2SiO_5 solution at 70 °C for 40 min and then rinsing in running cold water for 4 min, neutralization in a mixed solution of 1.2 g/l Na_2CO_3 and 0.4 g/l borax at 70 °C for 4 min, and drying in an oven at 100 °C for 30 min before enameling. The experimental conditions for each group of specimens is given in Table I.

Commercial frits 5205, 5206, and 5263 from Ferro Co., Japan, were ball-milled separately down to 200 mesh and mixed, with equal part of each frit and additives of kaolinite, quartz, borax, $NaNO_2$ and water, to form a batch of enamel slip. The specific gravity of the enameling slip was controlled between 1.6–1.67 by adjusting the water content, and the slip was aged for 36 to 48 h before enameling to improve its fluidity. The enamel slip was then applied to the pretreated sheet steel by a hand-spraying system. The weight gain for each specimen after enameling was about 33 mg/mm^2, resulting in a coating of thickness ∼100 μm. The specimens were then dried in an oven at 150 °C for 30 min. Firing of the porcelain enamel was carried out in a box furnace at 820 °C for 4 min and then cooled in air.

The adherence of porcelain enamel to steel was evaluated using a conventional method, the electrical conductivity measurement, which gives a percentage number called adherence index. This testing method was initiated in 1951 by the Porcelain Enamel Institute (PEI) of America and later in 1978 adopted by the American Society for Testing and Materials (ASTM) as a standard method for evaluation of the adherence of porcelain enamels and ceramic coatings to sheet metals [9]. Since then, it has been widely accepted by the enamel industry as a quality control tool for evaluation of the adherence of porcelain enamels to low carbon steel.

To prepare for the conductivity measurement, a circular depression is first made on an originally flat enameled sheet steel by a deforming press. In addition to cohesive failure where fracture of the enamel occurred owing to deformation, adhesive failure resulting from the delamination of the enamel from the steel substrate, can readily take place in systems where the bonding strength between enamel and steel is weak; thus the steel substrate is exposed to the air. After cleaning the loosely bound enamel fragments from the steel substrate, the electrical conductivity of the depressed region in the specimen is measured by an adherence meter.

The adherence meter is an electronic instrument equipped with 169 needle-like probes assembled in a hexagonal pattern. Each probe is connected to an electrical circuit, which will be completed through the grounded base metal of the specimen where the enamel (an insulator) is broken down completely and the base metal is in direct contact with the probe. Conductivity measurement is done by pressing the probe head against the depressed region of the specimen and counting the number of probes, X, which form complete circuits. The extent of adhesion between enamel and steel is expressed by an adherence index:

$$A = [(169 - X)/169] \times 100 \quad (1)$$

It can be easily understood that the higher the adherence index, the better the adhesion of the enamel to the steel.

The surface topography of the enameled specimens after aforementioned mechanical deformation was examined by an Olympus PME3 microscope. To understand the effect of different surface pretreatments on the microstructure of the enameled stainless steel and their influence on the adherence, cross-section specimens were prepared by a standard metallography procedure [10]. Examination of the interfacial microstructure was carried out by a JEOL 5400 scanning electron microscope (SEM) equipped with a Link energy dispersive spectrometer (EDS). The microscope was operated at an accelerating voltage of 15 kV and the electron micrographs were recorded using the backscattered electrons. The chemistry of the reaction products at the enamel-steel interfaces was analyzed both by an energy dispersive spectrometer which has energy resolution of 138 eV for MnK_α, and by glancing angle X-ray diffraction using CuK_α radiation with incident angle of 1°.

3. Results

3.1. Surface morphology of the stainless steel before enameling

An electron micrograph of the surface morphology of specimens treated with ball blasting is given in Fig. 1a, in which scratches and gouges due to mechanical damage can be readily seen. The surface appearance, in general, is rough and full of fiber-like debris. The surface finish of the two sides of the as-received steel plates is different: one is rough with rolling marks, Fig. 1b, and the other is relatively smooth, Fig. 1c, corresponding to the specimens of categories (ii) and (iii), respectively. The rolling marks on the specimens of category (ii) are mainly parallel to the rolling direction. After polishing with grit #1200 SiC paper and 1 μm Al_2O_3,

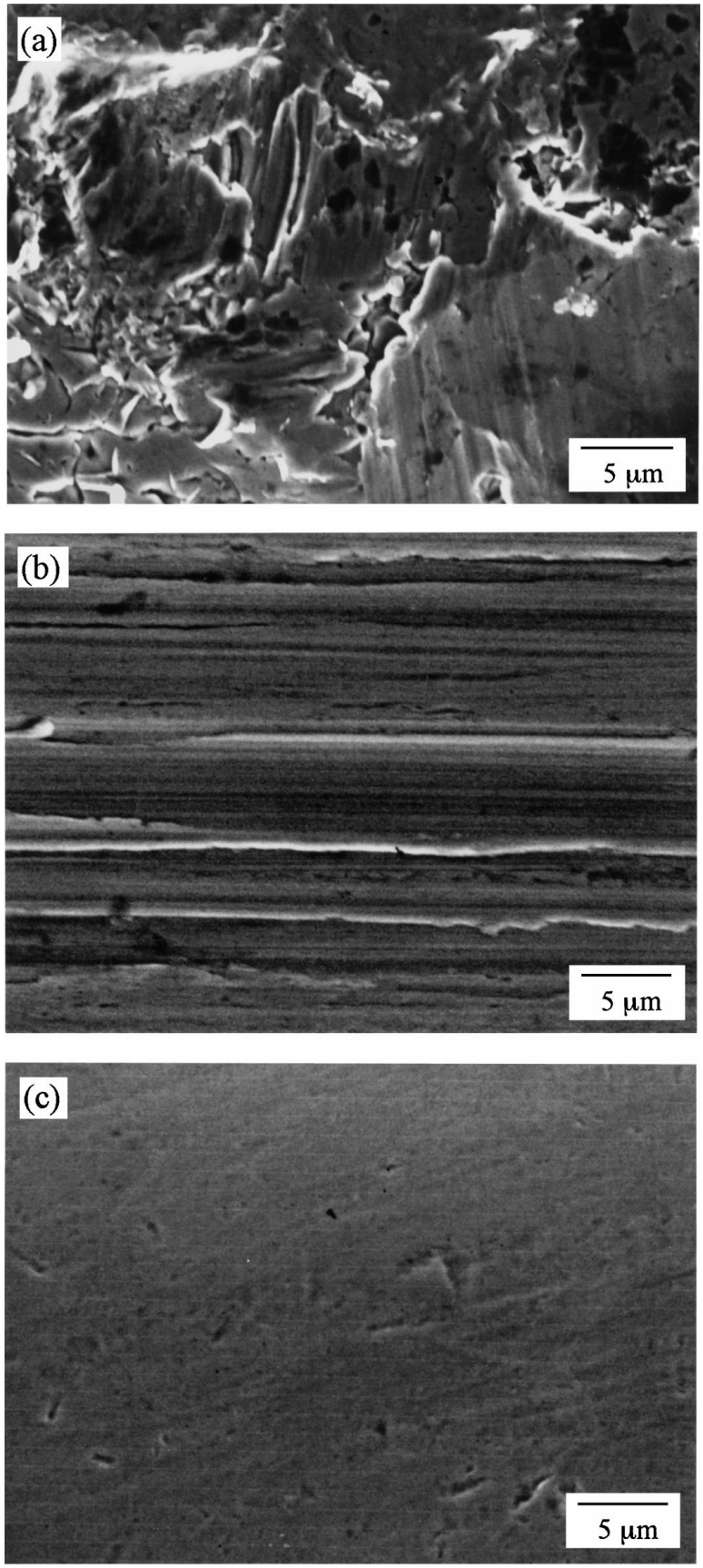

Figure 1 SEM micrographs of the stainless steel surface before enameling: (a) specimens treated with ball blasting, (b) as-received specimens with rolling marks, (c) as-received specimens with smooth surface.

some rolling marks still remain on the specimen surface. Although the smooth surface of specimens in category (iii) is optically reflective, a close look at Fig. 1c, indicates the presence of surface defects such as dents and voids. From the SEM observation, it is found that the surface of the specimens oxidized in air at 500 °C for 5 min remains pretty much the same as that of the specimens without oxidation treatment, except that the color of the specimens changes from silver gray to golden brown.

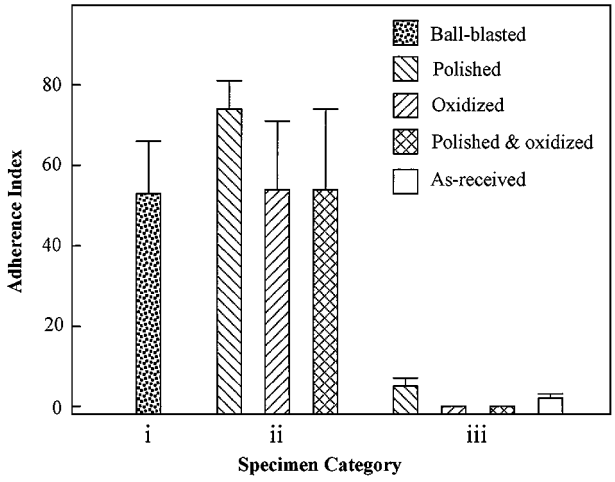

Figure 2 A histogram showing the measured adherence indices of porcelain enamel to the stainless steel with different surface pretreatments.

3.2. Adherence of porcelain enamel to the stainless steel

A histogram showing the adherence of porcelain enamel to steel for each category of the specimens is given in Fig. 2. It can be seen that specimens of categories (i) and (ii) exhibit much better adherence than those of category (iii). The adherence index of specimens in category (iii) is very close to zero, i.e., the enamel coatings are almost completely delaminated from the substrates and the steel is exposed to the air upon impact by the deforming press. As a result, the depressed area in the specimens of category (iii) gives a bright and lustrous appearance, as shown in Fig. 3a.

Unlike the specimens of category (iii), the depressed area in the specimens of either category (i) or category (ii) looks dull and rugged, as shown in Fig. 3b. After cleaning the loosely bound enamel fragments from the steel substrate, a close examination of the depressed area reveals that a large portion of the region is still covered by enamel remnants. It is noted that the area percentage covered by the enamel remnants increases with the value of the adherence index. The adherence index, 53 ± 13, of specimens in category (i) is lower than that, 61 ± 15, of the specimens in category (ii). In addition, among specimens of category (ii) of which the surface of the as-received steel substrates has rolling marks, final polishing of the substrates by 1 μm Al_2O_3 alone produces the highest bonding strength between the porcelain enamel and the steel.

3.3. Microstructure of enamel-steel interfaces

A cross-section SEM micrograph of the enamel-steel interface in which the steel was ball-blasted, is shown in Fig. 4a. As a result of the impact by the steel balls, the steel near the substrate surface was heavily deformed and large pieces of steel are displaced from its original position, resulting in the formation of wavefront-like morphology as illustrated in Fig. 4a. The microstructure of the enamel-steel interface of specimens, which were undergone oxidation treatment before enameling, in category (ii) where the surface of the as-received steel

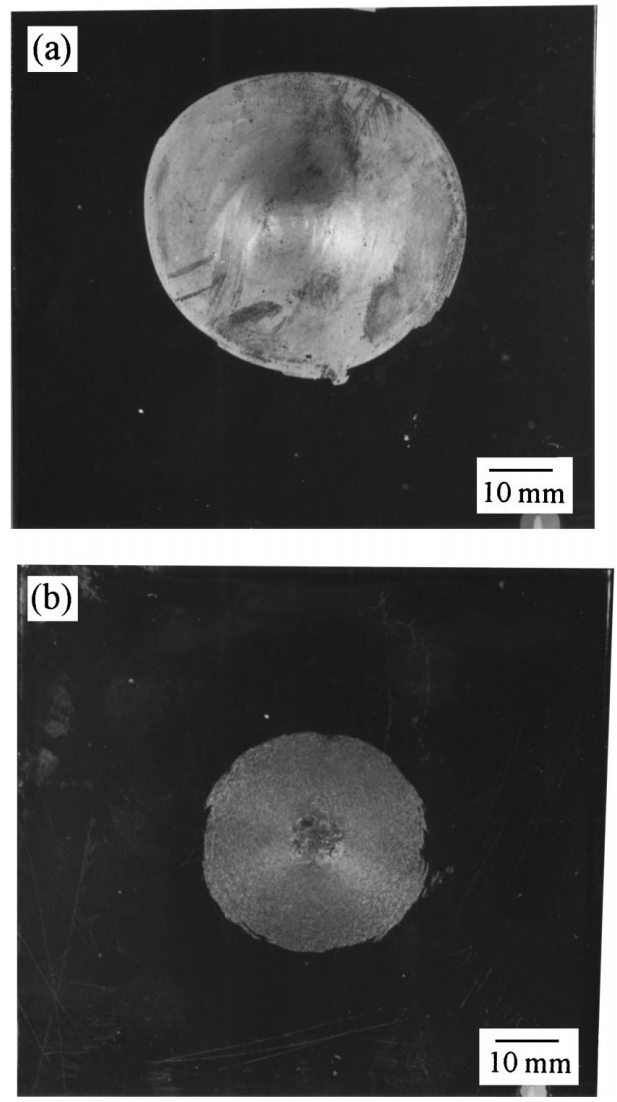

Figure 3 Optical micrographs of the enameled steel upon impact deformation for conductivity measurement, illustrating the different appearance of specimens with (a) poor and (b) good adherence.

substrates has rolling marks, is shown in Fig. 4b. The interfacial morphology of the specimens which were pretreated either polishing, oxidation or both, in this category is similar. A cross-section SEM micrograph of the enamel-steel interface of the as-received specimens in category (iii) is shown in Fig. 4c, from which it can be seen that the interface is rather flat.

Cross-section SEM result in Fig. 4 shows that the interfacial morphology of the enameled steel is different for specimens of different surface pretreatments. By taking the shortest contour length of the enamel-steel interface of the as-received specimens in category (iii) as a reference, the ratios of the contour length for each group of specimens are calculated and listed in Table I. The average contour ratios of categories (i), (ii), and (iii) are 1.48, 1.30, 1.03, respectively. In addition, it is noted that specimens of category (i), shown in Fig. 4a, has the longest interfacial contour length, i.e., highest contour ratio, due to the presence of wavefront-like morphology, but in practice, as indicated in Fig. 4b, the interfacial contour of the specimens in category (ii) is much uniform and the local roughness of the interface is higher than that of the specimens in category (i).

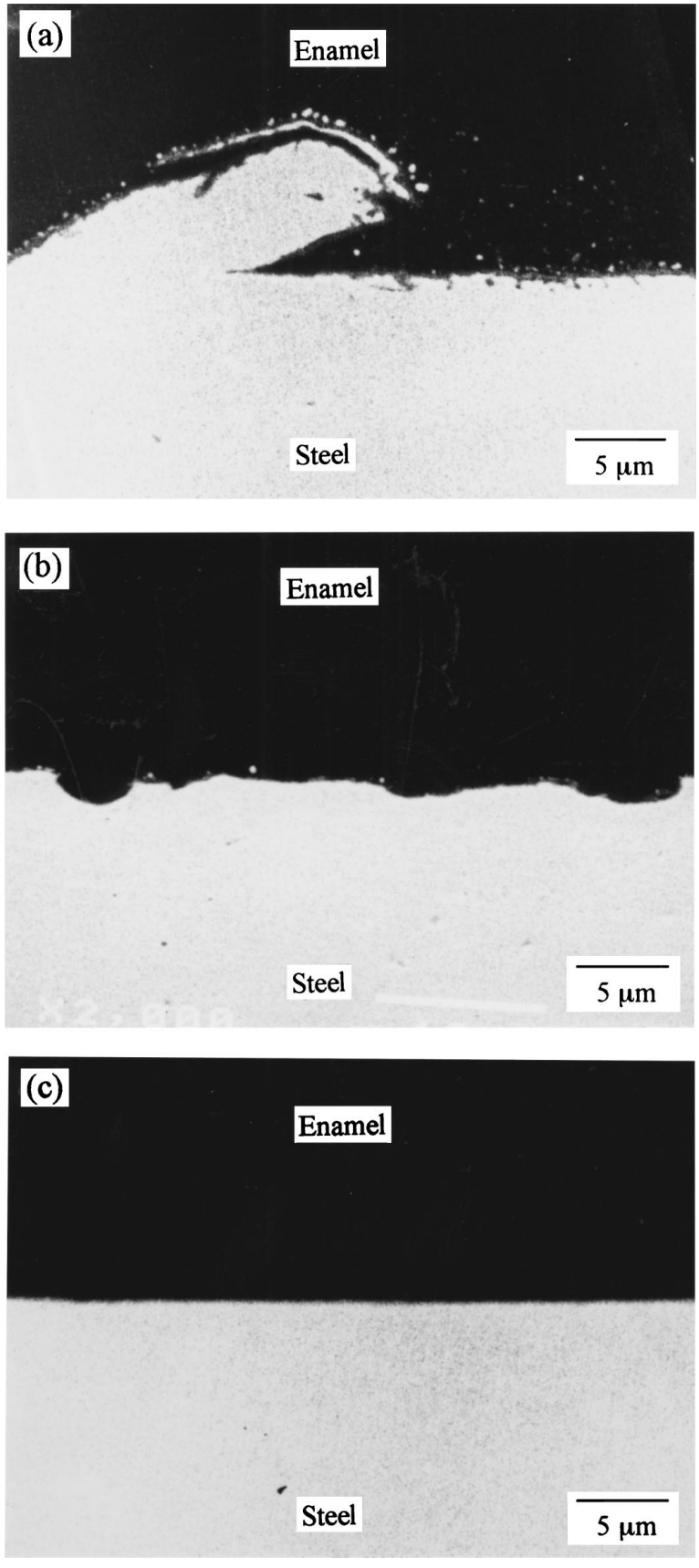

Figure 4 Cross-section SEM micrographs of the enamel-steel interfaces with different surface pretreatments: (a) the steel substrate was ball-blasted, (b) as-received specimens with rolling marks, (c) as-received specimens with smooth surface.

4. Discussion

4.1. Control of the adherence by a mechanism of mechanical interlocking

In the literature [3–6, 11, 12], two basic theories are proposed to describe the bonding mechanism of enamel-steel or -metal interfaces. One attributes adherence to the formation of chemical bonding at the interface, and the other considers it as a result of mechanical interlocking. Which mechanism controls the final bonding strength of enameled steels is still a subject of

controversy. Although, in principle, the chemical bonding which results from some various chemical reactions at interfaces, should give higher bonding strength, examples exist that excessive chemical reactions can deteriorate the bonding strength of the enamel-steel interfaces [3, 7].

Since no reaction layer between the enamel and the steel is observed from the SEM analysis, within the resolution limit of the microscope under operation, 10 nm, the interface morphology must play an important role in controlling the adherence of the enamel coatings to the steel. The experimental results of conductivity measurement shows that good adherence of the porcelain enamel to the steel is associated with those specimens that have high contour ratios, i.e., rough interfaces. A plot of the adherence index vs. the average contour ratio gives a sigmoidal curve, in which the adherence index reaches a saturation value of ∼60 as the contour ratio is higher than 1.30. The fact that all the specimens from category (iii) have very low adherence can be understood from the cross-section SEM micrograph in Fig. 4c, in which the interface is relatively flat and is lacking any mechanical interlocks. By increasing the interface roughness either by ball blasting (category (i)) or cold rolling during sheet steel forming (category (ii)), the adherence can be improved significantly. Similar results were reported by Richmond *et al.* [4, 5] for porcelain enameled plain carbon steel, in which nickel-flashing were used to introduce galvanic corrosion at the interface and thus produced many anchor points to enhance the adherence.

For specimens of category (ii) of which the steel surface has rolling marks, it is observed that polishing of the substrate with 1 μm Al_2O_3 results in better adherence than those pretreated with oxidation, and with both polishing and oxidation. The last two groups of the specimens involve an oxidation treatment of the steel substrates in air at 500 °C for 5 min before enameling; thus a thin layer of iron oxides is present at the enamel-steel interface (see next section). The chemistry of the enamel-steel interface in which the steel was oxidized before enameling is expected to be different from that of the specimens treated by polishing only. Surprisingly, the experimental result of conductivity measurement shows that oxidation treatment has no significant effect on the adherence, and no direct correlation between adherence index and the ratio of interfacial contour is found in this category of specimens. In fact, the polished specimens without oxidation treatment demonstrate the highest adherence among this category of specimens. This result gives a direct evidence that mechanical interlocking controls the adherence of the porcelain enameled stainless steel. It is, however, noted that this mechanism alone can enhance the adherence of the enameled stainless steel to a relative low level, i.e., adherence index ∼60, compared with that of plain carbon steels in which the adherence index up to 95 is readily obtained, in particular, using either nickel or cobalt flashing [3, 4, 7, 12]. Dietzel [13] proposed a galvanic corrosion mechanism to explain the roughening and high density of anchor points at the enamel-steel interface, and thus good adherence of the enameled plain carbon steels. Since the oxidation potential of the stainless steel is different from that of the plain carbon steels, this mechanism may not be applicable to the stainless steel. Indeed, the experimental results suggest that surface roughening either by ball-blasting or mechanical polishing is a more practical way of enhancing the adherence of enameled 316L stainless steel.

4.2. Adhesive failure of the enameled stainless steel

Formation of primary bonding resulting from chemical reactions at metal-ceramic interfaces has long being considered to be an important mechanism for enhancing the bonding strength of metal-ceramic interfaces [3, 11, 12]. The fracture surface of the enameled stainless steel with oxidation pretreatment upon impact deformation exposes the luster appearance of the metal, which suggests that delamination of the coating occurred between the steel substrate and the oxide layer produced during the oxidation pretreatment. Analysis of the delaminated enamel fragments by X-ray diffraction reveals the presence of α-Fe_2O_3 in the remnants, as shown in Fig. 5. The presence of an iron oxide layer at

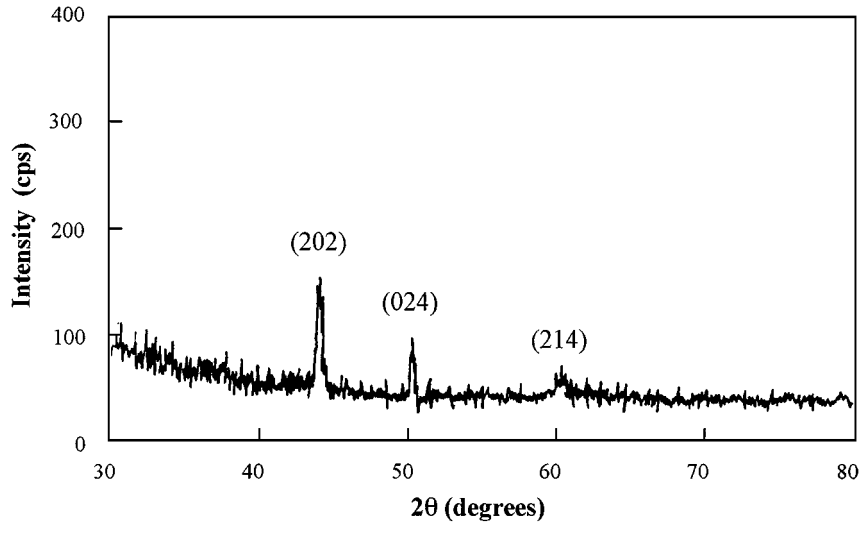

Figure 5 Glancing angle X-ray diffraction of the delaminated enamel fragments, in which the steel substrate was oxidized at 500 °C in air for 5 min before enameling, indicates the presence of α-Fe_2O_3 in the remnants.

the enamel-steel interface was also suggested by Ritchi *et al.* [14] from a comparison of the iron content across the interface using a chemical measurement and diffusion calculation. The atomic bonding between steel and its oxides is, in general, partly ionic and partly covalent, and has energies approximating the magnitude of 100 Kcal/mol, which is about an order of magnitude higher than the van der Waals bonds [15]. Nevertheless, it is observed from the experiment that failure of the enameled steel oxidized at 500 °C for 5 min before enameling occurred between the oxides and the steel. Similar result was reported by Hautaniemi *et al.* [16], in which failure of the porcelain enameled titanium oxidized at 800 °C in a vacuum of 6.65 Pa to produce an oxide layer of ∼0.2 μm, was found to occur between the metal and the oxide layer underneath the enamel.

It is known that chemical bonding between metal and ceramic produces much better adherence than mechanical interlocking, and is considered to be a more favorite bonding mechanism for metal-ceramic interfaces. However, from the current experimental result, it is obtained that all the specimens in category (iii) exhibit very poor adherence. The low bonding strength of the enameled steel suggests that formation of chemical bonding at metal-ceramic interfaces is not a sufficient condition for good adherence. Other factors, e.g., defects and the state of residual stresses at the enamel-steel interface, may play an important role in controlling the adherence of porcelain enamel to the steel.

From a study of the microstructure and chemistry of an air-oxidized 316L stainless steel by Shieu *et al.* [8], it was shown that the oxidation pretreatment of the steel produced an oxide film of ∼70 nm thick, which is free from detectable defects such as cracks and voids in the oxide layer. In addition, it was demonstrated that the corrosion resistance of the oxidized steel in a hot boiling 30% sulfuric acid solution was improved considerably, compared with the steel without an oxidation treatment. Defects near the oxide-steel interface are thus unlikely to weaken the adherence of the oxides to the steel. On the other hand, when dealing with a ceramic coating on metals, it is essential to consider the residual stresses due to a difference in the coefficients of thermal expansion between the two materials as temperature is changed [7, 17]. An estimate of the unrelaxed thermal stresses in a metal-ceramic bilayer can be obtained by solving equilibrium, compatibility, and constitutive equations. Following the approach of Shieu and Sass [17], the unrelaxed thermal stresses in the enamel, σ_{enamel}, and the steel substrate, σ_{steel}, are

$$\sigma_{\text{enamel}} = \frac{\Delta\alpha \times \Delta T}{\left[\dfrac{(1-\nu_{\text{enamel}})}{E_{\text{enamel}}} + \dfrac{h_{\text{enamel}} \times (1-\nu_{\text{steel}})}{h_{\text{steel}} \times E_{\text{steel}}}\right]} \quad (2)$$

$$\sigma_{\text{steel}} = \frac{\Delta\alpha \times \Delta T}{\left[\dfrac{h_{\text{steel}} \times (\nu_{\text{enamel}}-1)}{h_{\text{enamel}} \times E_{\text{enamel}}} + \dfrac{(\nu_{\text{steel}}-1)}{E_{\text{steel}}}\right]} \quad (3)$$

where $\Delta\alpha = \alpha_{\text{steel}} - \alpha_{\text{enamel}}$, $\Delta T = T_{\text{low}} - T_{\text{high}}$, and α, h, E, and ν are the coefficient of thermal expansion, thickness, Young's modulus, and Poisson's ratio of the materials, and T_{high} and T_{low} are the firing temperature of the enamel and the temperature after cooling down, respectively.

TABLE II Elastic constants of enamel, α-Fe_2O_3, and 316L stainless steel [18, 19]

Material	E (GPa)	ν	α ($\times 10^{-6}$ K^{-1})
Enamel	72.5	0.23	8.6
α-Fe_2O_3	51.1	0.26	9.0
Steel	193	0.28	18.4

By substituting the corresponding parameters for enamel and steel listed in Table II into the above equations, the unrelaxed thermal stresses in the enamel coating and the steel, upon cooling from the firing temperature of 820°C, are calculated to be 721 and 36 MPa, respectively. Since X-ray diffraction of the delaminated enamel fragments shows the existence of α-Fe_2O_3 adhered to the enamel, the enameled stainless steel is very likely to have a three-layer, i.e., enamel-oxide-steel, structure. According to the study of Brennan and Pask [11], oxides of iron tend to dissolve in porcelain enamel during firing; consequently, good compatibility is expected to exist between oxides and porcelain enamel. In addition, α-Fe_2O_3 has a coefficient of thermal expansion 9.0×10^{-6} K^{-1}, which is very close to that of the enamel, 8.6×10^{-6} K^{-1} [18]. Using Equation 2, it is calculated that the unrelaxed thermal stress in the oxide near the oxide-steel interface is 495 MPa. Since the resistance of a smooth enamel-steel interface, as shown in Fig. 4, to an applied shear stress parallel to the interface is weak, it is believed that failure of the enameled steel along the oxide-steel interface is assisted, to a large extent, by the residual thermal stresses resulting from the difference in the coefficients of thermal expansion between the oxide and the steel.

5. Conclusions

The adherence of porcelain enameled 316L stainless steel is dependent on the morphology of the enamel-steel interfaces. Specimens with rough surface before enameling, either produced by ball blasting or cold rolling during sheet steel forming, show much better adherence than those with smooth surface. For specimens of similar surface roughness, oxidation pretreatment resulting in a thin layer of oxide layer on the steel surface, does not have any significant effect on the adherence of the enamel coatings. It is therefore concluded that the adherence of porcelain enameled 316L stainless steel is mainly controlled by a mechanism of mechanical interlocking.

Acknowledgements

The authors would like to thank Mr. S. C. Lin of the China Steel Co., Taiwan, for his assistance in the conductivity measurement. Valuable discussions with Prof. S. L. Sass at Cornell University is gratefully appreciated. Financial support of this research by the National Science Council of Taiwan is acknowledged.

References

1. H. H. UHLIG and R. W. REVIE, "Corrosion and Corrosion Control," 3rd ed. (John Wiley & Sons, New York, 1985).
2. M. G. FONTANA, "Corrosion Engineering," 3rd ed. (McGraw-Hill, London, 1986).
3. B. W. KING, H. P. TRIPP and W. H. DUCKWORTH, *J. Amer. Ceram. Soc*. **42** (1959) 504.
4. J. C. RICHMOND, D. G. MOORE, H. B. KIRKPATRICK and W. N. HARRISON, *ibid*. **36** (1953) 410.
5. D. G. MOORE, J. W. PITTS, J. C. RICHMOND and W. N. HARRISON, *ibid*. **37** (1954) 1.
6. S. S. TSAUR, F. S. YANG, Y SHUEH, R. YOU and P. SHEN, *Mat. Sci. Eng*. **A165** (1993) 175.
7. F. S. SHIEU, K. C. LIN and J. C WONG, *Cream. Int*. **25** (1998) 27.
8. F. S. SHIEU, M. J. DENG and S. H. LIN, *Corror. Sci*. **40** (1998) 1267.
9. Annual Book of ASTM Standards, "Standard Test Method for Adherence of Porcelain Enamel and Ceramic Coating to Sheet Metal," Vol. 02.05, C313-78 (Philadelphia, 1983).
10. ASM Handbook, "Materials Characterization," Vol. 10, 9th ed. (American Society for Metals, 1986).
11. J. J. BRENNAN and J. A. PASK, *J. Amer. Cream. Soc*. **56** (1973) 58.
12. E. PAPARAZZO, G. FIERRO, G. M. INGO and S. STURLESE, *ibid*. **71** (1973) C-494.
13. A. DIETZEL, *Ceram. Abstr*. **13** (1934) 250.
14. D. RITCHI, H. A. SCHAEFFER and D. WHITE, *J. Mater. Sci*. **18** (1983) 599.
15. L. H. VAN VLACK, "Physical Ceramics for Engineers" (Addison-Wesley, London, 1964).
16. J. A. HAUTANIEMI, H. HERO and J. T. JUHANOJA, *J. Mater. Sci*. **3** (1992) 186.
17. F. S. SHIEU and S. L. SASS, *Acta Metall. Mater*. **39** (1991) 539.
18. V. V. VARGIN, "Technology of Enamels" (Maclaren and Sons, London, 1967).
19. G. E. DIETER, "Mechanical Metallurgy" (McGraw-Hill, London, 1988).

Received 31 July 1998
and accepted 4 May 1999